Published in final edited form as:

IEEE Int Conf Connect Health Appl Syst Eng Technol. 2023 June ; 2023: 22–33.

FoG-Finder: Real-time Freezing of Gait Detection and Treatment

Kenneth Koltermann,
Department of Computer Science, William & Mary

Woosub Jung,
Department of Computer Science, William & Mary

GinaMari Blackwell,
School of Nursing, Virginia Commonwealth University

Abbott Pinney,
Department of Computer Science, William & Mary

Matthew Chen,
Department of Computer Science, William & Mary

Leslie Cloud,
Department of Neurology, Virginia Commonwealth University

Ingrid Pretzer-Aboff,
School of Nursing, Virginia Commonwealth University

Gang Zhou
Department of Computer Science, William & Mary

Abstract

Freezing of gait is a serious symptom of Parkinson's disease that increases the risk of injury through falling, and reduces quality of life. Current clinical freezing of gait treatments fail to adequately address the fall risk posed by freezing of gait symptoms, and current real-time treatment systems have high false positive rates. To address this problem, we designed a closed-loop, non-intrusive, and real-time freezing of gait detection and treatment system, FoG-Finder, that automatically detects and treats freezing of gait. To evaluate FoG-Finder, we first collected 716 freezing of gait events from 11 patients. We then compared FoG-Finder against other real-time systems with our dataset. Our system was able to achieve a 13.4% higher F1 score and a 10.7% higher overall accuracy while achieving a reduction of 85.8% in the false positive treatment rate compared with other validated real-time freezing of gait detection and treatment systems. Additionally, FoG-Finder achieved an average treatment latency of 427ms and 615ms for subject-dependent and leave-one-subject-out settings, respectively, making it a viable system to treat freezing of gait in the real-world.

Keywords

freezing of gait; neural networks; wearable devices

1 Introduction

Over 10 million people in the world have Parkinson's Disease (PD) with an estimated 90,000 new diagnoses per year (up from 60,000) in the United States alone [51]. Roughly 60% of PD individuals experience Freezing of Gait (FoG), a potentially dangerous symptom of PD. FoG is the abrupt stoppage of normal gait wherein the individual is unable to take effective forward steps. FoG can also result in decreased forward and lateral stability. The risk of falling and sustaining serious injury as a result of FoG increases with the progression of the disease over time [29]. For this very reason, FoG is dangerous and results in a lower quality of life for those with PD.

At present, PD is incurable but treatments exist to reduce the severity of FoG symptoms. Current clinical treatments include medications such as Carbidopa-Levodopa [48] or deep brain stimulation surgery (DBS) [41] which may reduce the severity and frequency of FoG events, but the risk of falling will still remain. Other treatments that currently exist require manual user input [11] or provide constant cuing [32]; since FoG is sudden and may give no warning, these treatments are inadequate to address the fall risk posed by FoG symptoms. Vibration therapy and auditory cuing can reduce the severity of FoG symptoms or fully abort FoG events when they occur [1, 22, 38, 52]. However, habituation where the patient becomes accustomed to these treatments can reduce treatment efficacy if these treatments are activated too often or in predictable sequences. As such, there is a clear need for an accurate, non-intrusive, and portable real-time FoG detection system for automatic, real-time treatments to be effective. The need for such a system leads us to our main research question: **How can we accurately detect and treat FoG events in real-time?**

To answer this research question, we developed FoG-Finder, a closed-loop, non-intrusive, and portable FoG detection and treatment system consisting of Inertial Measurement Unit (IMU) sensors, a smartphone, and vibration therapy devices. To accurately detect FoG, we first generated additional time-series features to address different ways patients can freeze. We transform our time-series features into the frequency domain using separate Butterworth (BW) filters to extract information for frequency bands that dominate normal gait cycles and FoG events. We then used a multi-input Convolutional Neural Network (CNN) model in order to allow our model to capture patterns within the normal gait frequency band and FoG event frequency band separately.

To evaluate our system, we collected data from 11 PD patients from May 2021 to present in an IRB approved study. To the best of our knowledge, our dataset is the most FoG-rich IMU sensor dataset to date with over 700 clinically labeled FoG events. Our dataset was designed to capture a wide variety of FoG events from the 5 most common FoG triggering scenarios. We evaluated our work against other real-time FoG detection and treatment systems using our dataset, and demonstrate that our system provides a significant performance boost of 13.4% higher F1 score and 10.7% higher overall accuracy over existing FoG detection and treatment systems in a leave-one-subject-out (LOSO) scenario.

FoG detection is a heavily studied area of research with many works proposing different detection methods. However, few works focus on detection in real-time and even fewer

demonstrate their methodology is capable of functioning in real-time using portable hardware. Bachlin et al. [4, 5] proposed what we believe to be the first functional real-time FoG detection and treatment system, using thresholding of frequency powers to detect FoG symptoms. They achieved 73.1% and 81.6% sensitivity and specificity, respectively, on their 10 patient dataset (DAPHNET) in a LOSO setting. Mazilu et al. [26] used time domain and frequency domain features with adaboosted C4.5 trees to achieve 66.3% and 95.4% sensitivity and specificity, respectively, with the DAPHNET dataset under LOSO conditions. Both Bachlin and Mazilu use features that condense temporal data down to singular values which results in a loss of information. Our work uses BW filters to extract useful frequency information while maintaining the temporal nature of the data. Naghavi et. al [30] proposed their DGAD system in 2021 which used a single BW filter on time-series data and a deep CNN to detect FoG. They achieved 63.0% and 98.6% sensitivity and specificity, respectively, on their 7 patient dataset in a subject-dependent setting. Different from DGAD, FoG-Finder separates the normal gait and FoG frequency bands for input to our CNN model, improving it's ability to distinguish FoG events. What separates these works from many other FoG detection papers is that their methods are proven to be real-time on portable computing systems, and therefore practical for real-world application. We faithfully implemented their respective methods and compared their works against FoG-Finder using our dataset. Compared with these works, FoG-Finder achieves 13.4% higher F1 score and 10.7% higher overall accuracy while achieving a reduction of 85.8% in the false positive treatment rate.

Our contributions are summarized as follows:

- We devised a close-loop, portable system with a real-time evaluation that was deployed over several months and is accepted by patients.
- We filtered our IMU data with separate BW filters to extract frequency data for the typical gait frequency and FoG frequency bands whilst still maintaining the temporal nature of the data. We input these frequency bands into our CNN model separately which improves performance over related works that combine frequency band data.
- Our system design provides a performance increase of 13.4% higher F1 score and 10.7% higher overall accuracy compared to other real-time FoG detection systems when evaluated under a LOSO setting.
- Our FoG dataset is the most FoG-rich dataset to date with at total of 716 FoG events across 11 patients and contains freezes from the five most common FoG triggering scenarios. We are still collecting data from new patients through 2023, and our dataset will be made publicly available upon the conclusion of our study.

The remainder of this paper is structured as follows: Section 2 describes a high-level view of our FoG detection and treatment system. Section 3 provides details about the specific features we chose to use for FoG detection. Following this, Section 4 describes our FoG detection model design. Next, we provide information about our clinical data collection process and testing protocols in Section 5. We then compare our work against other real-time

FoG detection systems with a robust performance evaluation in Section 6. Section 7 contains a detailed related work. Finally, we conclude the paper in Section 8.

2 Real-time FoG Detection and Treatment System

There are several requirements for real-time FoG detection and treatment systems to be viable. First, systems must be non-intrusive and portable in real-world environments. Second, systems need fast and real-time FoG detection. The latency from FoG onset to treatment must be below 1s to prevent falls, but faster treatment activation is desirable. Finally, systems must be in-situ: if FoG occurs, then the system must detect and treat the event. Failing to detect an FoG event could result in the patient falling and sustaining injury.

Our system consists of three main components: IMU sensor bands, vibration treatment devices, and an Android smartphone. Figure 1 provides a high-level overview of our closed-loop system.

IMU sensor bands:

For FoG-Finder, we used the Ultigesture (UG) wearable IMU sensor platform [54]. The UG platform samples data at a rate of 100Hz, contains a 3-axis accelerometer and 3-axis gyroscope, and is smartphone compatible using Bluetooth (BT). Additionally, the UG devices are inexpensive, costing around $10 each. A desired, but not required aspect would be for FoG-Finder to fulfill the important requirements listed above while also remaining inexpensive for patients. Patients wear a UG device on each ankle.

Vibration Treatment Device:

The vibration treatment device is the PDVibe3 [1, 52]. The device is ankle worn and provides vibrotactile treatment directly to the feet of the patient. Vibration therapy has been shown to be an effective FoG treatment in reducing the frequency and severity of FoG symptoms [22, 38].

Android Smartphone:

We use an Android smartphone, the Google Pixel 4a, as the portable computer which processes the IMU data stream sent via BT. The smartphone contains our FoG detection neural network which performs the FoG classification. Should FoG be detected, the smartphone activates the vibration treatment. Our FoG-Finder application requires no user input or communication with any cloud device in order to detect and treat FoG making it suitable for real-world environments.

Figure 2 provides an overview of the flow of data within the smartphone. Our app uses the most recent 1.28s of data from the left and right UG data streams; these 1.28s windows of data are first normalized separately before being combined and filtered with two different BW bandpass filters for the normal gait and FoG frequencies. These two filtered windows are inputted separately into our CNN model. To ignore singular erroneous predictions, we used consecutive class post-processing to determine if treatment should be activated.

The UG devices and PDVibe3s are placed on the ankle about 45° outward from the rear of the ankle. Figure 3 shows this placement on the ankle. This placement is non-intrusive for the patient and the devices can easily be hidden under pants or socks to remain inconspicuous. Section 6.4 of the evaluation provides details about patient responses to questions about device comfort. Vibration therapy can be applied directly to the sensitive locations of the foot rather than another part of the body. We placed an IMU on each ankle because FoG symptoms may appear on only one foot, otherwise known as asymmetric freezes. During an asymmetric freeze, one foot is capable of taking effective steps forward while the other foot cannot be effectively picked up. We want to capture information from both feet to account for this possibility.

3 FoG Detection Feature Extraction

3.1 Time Domain Features

There are six sensor readings recorded every 10ms (AX, AY, AZ, GX, GY, GZ) per IMU. For each group of six sensor readings, we compute the magnitude of the acceleration and gyroscope signals using the standard magnitude formula provided below:

$$Mag(X, Y, Z) = \sqrt{X^2 + Y^2 + Z^2} \quad (1)$$

Additionally, we compute the magnitude of the acceleration and gyroscope without the Y component. Mag(AX,AZ) provides information useful for identifying pivot turns – turns where the patient slides their feet on the floor to rotate without lifting their heels. Mag(GX,GY) is useful for straight path FoG freeze detection, especially since straight path freezes are less common than turn freezes in our dataset. The result of these new feature computations is 10 data points per IMU every 10ms.

For training FoG-Finder models, we chunk the data stream into 1.28s windows with a step size of 20ms. We chose 1.28s as the window size because 1.28s is long enough to capture a full gait cycle, but short enough to not include redundant past gait information. Additionally, previous works studying FoG have determined that while smaller window sizes yield reduced per-window performance, it also tends to yield lower latency for FoG detection [26].

We normalize the left and right UG data separately because PD is often accompanied by other gait deficiencies such as ataxia, dystonia, and dyskinesia [12, 14, 44]. These deficiencies may lead to patients having different gait cycle characteristics for each leg. Additionally, we normalize each patient's data individually rather than normalizing all patient data together. The primary reason we do this is to avoid the compression of patient data. Patient characteristics such as leg length, stride length, and stride speed influence a patient's gait pattern.

The FoG-Finder model described in Section 4 is a CNN-based architecture. The data from each UG device is temporally related – ie: it is important for our CNN model to learn that the left and right UG streams are connected by time. To achieve this, we combine the left and right UG data in a way that the convolutional windows of our FoG-Finder models

capture left and right sensor axes together. Figure 4 provides a visual describing this process. When this process is complete, we end with a data shape of (128,20,1) for each window. Windows that had 30% or more overlap with FoG time segments were labeled as FoG.

3.2 Frequency Domain Features

Moore et al. [28] showed that two distinct frequency bands exist for normal gait cycles and FoG events. Normal gait cycles typically have a dominant frequency within 0.5–3Hz while FoG events typically have a dominant frequency between 3–8Hz. It is understood that the frequency pattern identified by Moore et al. persists between different PD patients experiencing FoG even with different gait characteristics. As such, inclusion of frequency domain features is important for FoG detection for LOSO analysis.

We use 5th order BW bandpass filters with the Morlet wavelet pattern to extract frequency domain data from the time domain. We chose BW filters because they capture frequency information from time-series data while being less computationally expensive as FFT or CWT since fast execution time is important. We use a 0.5–3Hz BW bandpass filter on our time-series data which generates a new (128,20,1) shape containing filtered gait frequency band data. We also use a 3–8Hz BW bandpass filter on our time-series data separately to generate data of shape (128,20,1) which contains information pertaining to the FoG frequency band.

4 FoG Detection Model Design

We elected to use a multi-input CNN-based architecture for FoG detection for two reasons. First, convolutional layers are fast, an order of magnitude faster than long short-term memory (LSTM) neural networks [50], which is important since our model must be fast to ensure we maintain low FoG detection latency on mobile hardware. Second, CNNs capture special relationships between data from different points in time making them suitable for FoG detection. Figure 5 provides an overview of our FoG-Finder model. Our model consists of two separate sections each consisting of three convolutional layers. Features generated by convolutional layers become more complex with each layer with the features of the first convolutional layer being more generalized than later layers. FoG detection is an inherently hard problem because of the many different ways patients can experience FoG. Therefore, we chose three convolutional layers because our network is deep enough to capture more complex patterns associated with FoG while still maintaining low computation time. Additionally, there is a low risk of experiencing the vanishing gradient problem with just three convolutional layers.

Since feature representations become more complex with CNN depth, we double the number of filters used after each convolutional layer. The increased number of filters with CNN depth allows our model to capture more unique representations of the features. Between each convolutional block containing a convolutional layer, batch normalization, and ReLU activation, we perform max pooling to down-sample the features which helps reduce computation time of the later layers of our model as well as reduce over-fitting. Past works with frequency thresholding [4, 5, 16, 28] found success and insight into FoG detection by looking at the gait frequency and FoG frequency bands independently. We applied this

principle when developing our model. We input the gait frequency band and FoG frequency band data into the model separately in order to allow the model to extract features for each of these frequency bands independently. As we will show in Section 6, this architecture out-performs real-time FoG detection systems that use either frequency thresholding or use CNN models that combine these frequency bands.

To avoid singular, erroneous FoG classifications from the FoG-Finder model triggering treatment, we use N consecutive FoG classifications to determine if treatment should be activated. For our study described in Section 5, N is 2. A lower N leads to less latency from FoG onset to treatment with the possibility of more false treatments while a higher N leads to more treatment latency with fewer false treatments. The execution time for our CNN model is <35ms and the execution time to generate our BW features is under <25ms. In total, the execution time of FoG-Finder is <60ms per window.

5 Clinical Data Collection

5.1 Patient Demographics and Selection

Patients were admitted to our study with the goal of collecting a large, FoG-rich dataset containing FoG events initiated by the top five FoG triggering scenarios [20]. A FoG triggering scenario is an environmental or circumstantial factor that leads PD patients to freeze. The five most common FoG triggering scenarios are show in Figure 6 and are listed as follows: 6a: 540° turns, 6b: dual tasking (such as counting down from 100 by 7s while walking), 6c: walking through a narrow archway, 6d: walking towards a visual target (such as a chair to sit down), and 6e: time sensitive tasks (such as walking towards a ringing phone).

To be admitted to our study, patients must have been diagnosed with PD and experience FoG events triggered by at least two of the five FoG triggering scenarios. Table 1 provides an overview of the FoG events collected from the patients in our study. In total, we have collected 716 FoG events with a mean freeze time of 5.746s and median freeze time of 3.378s.

5.2 Data Collection Protocol

5.2.1 Test Environment Design—When designing our test environment, we wished to avoid problems present in past FoG datasets. It is common for past FoG datasets to be heavily imbalanced with the amount of non-FoG time greatly exceeding that of FoG time. Additionally, some FoG datasets lack protocols designed to collect FoG events caused by specific FoG triggering scenarios. It is not known at this time if FoG events induced by different triggering scenarios are distinguishable. Therefore, it is important that FoG datasets include a diverse range of triggering scenarios since a “narrow” dataset focusing on just one or two triggering scenarios may falsely give the impression that models evaluated on it are suitable for diverse scenarios.

Our test environment was specifically designed to induce as many FoG events as possible in a short amount of time. Unlike other datasets such as DAPHNET [4], we do not have a simulated daily living part of our study; we do this for several reasons. First, the scenarios in

our study are used by our clinicians assess FoG symptom severity and track PD progression in patients. Second, unstructured tests may lead to long segments absent of FoG since patients can avoid environmental factors that cause them to freeze. Our protocol allowed us to collect significantly more freezes than previous FoG datasets. Our dataset was collected in two phases as part of our study. All tests were conducted under an approved IRB protocol, IRB-HM20020085. Below, we will explain the purpose of each phase along with the characteristics of the protocols used for each phase.

5.2.2 Phase 1 Protocol—In Phase 1, data was collected from 6 patients in 2021. Each patient completed one visit and no vibration treatment was provided. These visits were short with each patient walking less than 10 minutes primarily because of COVID-19. Patients walked on a narrow Protokinetics ZenoMat [23] in a large physical therapy room. The ZenoMat is slightly softer than the floor of the room, and the data collected by the ZenoMat was not used for this specific study. Patients completed up to 8 short walks with the longest walk being two minutes. Each walk contained at least one FoG triggering scenario. Patients had no restrictions for footwear or clothing during each test. To ensure that we collected data for both left and right turns, Phase 1 contained two walking tests which specified which direction patients should turn.

5.2.3 Phase 2 Protocol—Patients completed two visits in Phase 2. Visit 1 was used to collect data to train a subject-dependent model, and visit 2 was for autonomous FoG detection and treatment. Patients that did not freeze in at least 2 of the 5 FoG triggering scenarios or froze less than 5 times during visit 1 were removed from the study. Our goal is not only to build robust subject-dependent models, but also to capture as many FoG events from each FoG triggering scenario so that future FoG detection systems may be evaluated against a diverse range of freezes. Figure 6 provides diagrams detailing the environment setup for each test used in Phase 2. During visit 1, each patient completed five 2-minute walks where each walk contained a different FoG triggering scenario. During visit 2, each patient completed 3 rounds of five 2-minute walks with FoG-Finder activating treatment when FoG was detected.

Patients wore both the UG sensor bands and PDVibe3 devices during both visits. We had patients wear the PDVibe3 devices during the first visit so that they could get used to walking with the devices attached to their ankles. Shoes and socks were provided to the patients during Phase 2 to ensure the shoes could accommodate the vibration tactors from the PDVibe3s, but patients had no other clothing restrictions. If a subject wore pants, they could elect to wear the devices outside or inside their pants or roll their pants up. This freedom is meant to reflect how clothing could impact the resting position of the UG sensors according to patient preferences during real-world deployment. For treatment during Phase 2, the system would apply 2 seconds of vibration followed by 1 second of downtime before the next vibration treatment could be applied. 2 seconds of vibration was chosen because vibration has a cumulative and immediate effect [22, 38].

5.3 Clinical Data Labeling

Differences in clinical FoG data labeling can make direct comparisons between FoG detection works using different FoG datasets difficult. First, there is no defined video labeling standard for clinical labeling of FoG which is used by all PD research groups, especially for how timestamps are assigned for the start and stop of FoG events. As such, different methodologies for FoG label assignment can have a significant influence on treatment latency evaluations and overall FoG detection model performance. Works unveiling a new FoG dataset should describe the data labeling process such as the number of labelers, the method for consensus building, and the specific criteria for identifying FoG and assigning start and stop labels. For our FoG dataset, we use the protocol defined by Dr. Gilat [15] in 2019 which is a revised version of the definition of FoG provided by Nutt et al. [33] in 2011.

FoG Start Identification:

Timestamp when the patient is no longer able to take effective forward steps with one or both feet while maintaining the intention of walking. Patient is displaying symptoms of FoG such as trembling, shuffling, or akinesia.

FoG End Identification: To affirm that FoG has ended, the patient must take at least two consecutive, effective alternating steps without displaying symptoms of FoG. Timestamp the initial toe-off of the first effective step in the sequence of consecutive, effective steps. Note: If one foot is able to take effective steps forward while the other foot displays symptoms of FoG, it is considered the same FoG event.

Consensus Building: Two experienced PD clinicians (20+ years of clinical experience with PD patients) labeled our dataset with two additional researchers present for annotation. Discussion of a potential FoG event continued until both PD clinicians were in agreement about a label.

Abnormal Gait: FoG events are not always easy to distinguish from abnormal gait. For the few events that were deemed a “toss-up”, the question “Would the patient benefit from treatment?” was used as a tie-breaker wherein if the answer was “Yes”, then the event was labeled as FoG.

6 Evaluation

In this section, we detail the factors that make comparison between different FoG detection works difficult and explain the most important evaluation criteria for evaluating FoG detection systems. We then compare FoG-Finder against other validated, real-time FoG detection works under subject-dependent and LOSO settings using our dataset.

6.1 Evaluation Methods

There are several factors that make direct comparison between different FoG detection works difficult. Below is a list of factors we believe need to be described in detail when comparing different FoG detection works:

1. Different methods for assigning non-FoG and FoG labels to windows (such as the % of FoG required for a window to be labeled as FoG).
2. Different window sizes as input for FoG classification (such as comparing results from models using 1s windows to models using 4s windows).
3. Inclusion/exclusion of windows containing both non-FoG and FoG data (exclusion is expected to increase performance).
4. Diversity of FoG events present in the evaluation dataset.
5. The use of different performance metrics. For performance metrics, there are three types of performance evaluation for window-based FoG detection systems: FoG window level, FoG event level, and treatment latency.

FoG Window Level Evaluation: FoG window level evaluation concerns each individual classification made by a model for windows of a fixed size W. Important metrics to provide are precision, recall, and F1 score because FoG datasets are usually heavily imbalanced favoring non-FoG time. Overall accuracy should also be reported. Finally, the false positive windows rate should be shown to provide information about how much error at the per window level is expected over time. Some methods may achieve high FoG recall at the expense of FoG precision which will lead to a high false positive treatment rate when evaluating at the FoG event level.

FoG Event Level Evaluation: FoG event level concerns model performance in detecting each FoG event which span multiple windows. It is important to show FoG event detection accuracy - the number of FoG events detected by the system against the number of FoG events labeled by clinicians - to gauge how many freezes would be left untreated by the system. Furthermore, since habituation is a risk for real-time treatments, the false positive treatment rate should be shown to identify how many unneeded treatments are likely to be applied over time.

Treatment Latency: Treatment latency concerns the time it takes for a system to treat a FoG event from the onset of the event. Generally speaking, a system should activate treatment within 1s of FoG onset to have the possibility of preventing a fall.

We have identified three main works that not only proposed FoG detection and treatment systems, but also validated their systems on portable hardware to prove that they are suitable for real-world deployment. These works are Bachlin et al. [4, 5], Mazilu et al. [26], and DGAD [30]. We provide a detailed explanation of these works in Section 7.1. To ensure that our evaluation against these works is robust and unencumbered by the evaluation factors listed above, we faithfully implemented these systems according to the specifications provided in their respective manuscripts so that they may be evaluated on our dataset. Additionally, we ensured that feature generation for each system used 1.28 windows of data so that the FoG window level performance evaluation was comparable between their works and ours. The method of assigning non-FoG and FoG labels to data windows was kept the same for all works.

6.2 Subject-Dependent Evaluation

Subject-dependent FoG modeling involves training and testing with data from the same patient. As such, performance is expected to be higher for models trained in this fashion over LOSO. In order for a subject-dependent evaluation to be valid, temporal consistency of the data must be maintained at the per-window level - ie: the training and test sets must not contain overlapping windows. This is a form of data leakage since overlapping windows will share the same feature space. This form of data leakage is unfortunately present in many past FoG detection works. To solve this problem for Phase 2 patients, we include the entirety of the patient's visit 1 data in the training/validation sets while the entirety of the patient's visit 2 data is reserved for testing.

For FoG-Finder and DGAD, the training/validation sets consisted of a 90/10% split for the data from all other patients and visit 1 of the test patient. Temporal consistency is maintained for non-FoG and FoG events during the generation of the training and validation sets. The training and validation loss was closely monitored for these models to ensure they did not overfit. Class weights were used to address the imbalanced nature of our dataset since only 40% of our dataset is FoG. The training set for Mazilu includes only visit 1 from the test patient to mirror the the way their system was trained in their work. Since Bachlin's method uses frequency thresholding for FoG detection instead of machine learning, visit 1 was used to determine the optimal threshold for FoG detection for each patient.

6.2.1 FoG Window Level Accuracy—Figure 7 shows the precision, recall, F1 score, and overall accuracy of FoG-Finder compared with Bachlin, Mazilu, and DGAD. Figure 8a compares the false positive window rate between FoG-Finder and these works. FoG-Finder achieves a 9.0%, 28.8%, 8.5% higher F1 score and 6.1%, 22.9%, 7.6% higher accuracy than Bachlin, Mazilu, and DGAD, respectively, while maintaining a reduction of 67.4%, 523.2%, 248.1% in the false positive window rate for these works, respectively. DGAD uses a 5 convolutional layer model with the raw time-series data (AX,AY,AZ,GX,GY,GZ) filtered with a single 0.5–8Hz BW filter. Since DGAD does not separate the gait band and frequency bands like FoG-Finder and does not use additional features designed to distinguish certain aspects of human gait, DGAD falsely predicts normal gait as FoG significantly more often than FoG-Finder. These figures show the performance of each of the systems without post-processing (if applicable) to determine if treatment is activated. Post-processing is utilized for FoG event level performance below.

6.2.2 FoG Event Level Accuracy—For FoG event level detection, post-processing is used after model classification to determine if treatment should be activated for FoG-Finder and Mazilu. FoG-Finder uses consecutive class post-processing described in Section 4. Mazilu uses the majority of the last 15 window classifications to decide if FoG occurred. DGAD and Bachlin do not have a method of post-processing after classification.

Habituation is a serious issue for vibrotactile and auditory FoG treatments because if a treatment is activated too often when not needed, there is a serious risk that the patient will become accustomed to the treatment and subconsciously ignore it. To reduce this risk, it

is desirable to reduce the false positive treatment rate while maintaining high FoG event accuracy and low treatment latency.

Figure 8b shows the number of correctly identified and treated freezes each real-time system. Figure 8c shows the FPTR of each system using the treatment protocol described in Section 5.2.3. All systems had comparable performance for identifying and treating true positive FoG events, but FoG-Finder achieved this performance while maintaining a 182.9%, 212.6%, 143.4% reduction in the average false positive treatment rate over Bachlin, Mazilu, and DGAD, respectively.

6.2.3 Treatment Latency—Treatment latency is the time difference between the timestamp for FoG onset of according to the clinical label and the time a system would activate treatment. Figure 8d compares the latency from FoG onset to treatment activation of FoG-Finder against Bachlin, Mazilu, and DGAD under subject-dependent conditions. Our average treatment latency in a subject-dependent setting is 427ms. To recap, it takes <60ms to create our BW features and perform a single FoG classification using our CNN model as stated in Section 5. The rest of the latency time comes from waiting until an adequate amount of FoG time has occurred for FoG-Finder to accurately identify an FoG event has started. This 427ms latency is only +78ms over the lowest average latency of 349ms achieved by DGAD. We believe that this small increase in latency over DGAD is acceptable given that FoG finder achieves a reduction in false positive treatment rate of 143.4%. Given these results, we purport that FoG-Finder achieves the requirement of being fast and real-time under subject-dependent conditions. Mazilu's latency of 1219ms is significantly larger than our work due to their method of post-processing using a majority vote for the last 15 classifications. Bachlin and DGAD have similar treatment latency's to FoG-Finder, but have significantly higher false treatment rates. We believe this is the case because our system has features designed to address normal turns where the patient only minimally lifts their ankle.

6.3 Leave-One-Subject-Out Evaluation

For LOSO analysis, data from one patient is reserved for testing while the data for all other patients is used for training and validation. The only patient not used for LOSO testing is P6 because they did not have any FoG events. For a LOSO evaluation to be valid, no data from the test patient may be used for training as this would otherwise be a subject-dependent evaluation. For Phase 2 patients, we complete our LOSO analysis using visit 1 since patients in Phase 1 completed only one visit.

6.3.1 FoG Window Level Accuracy—Figure 9 compares the LOSO window level performance of FoG-Finder against Bachlin, Mazilu, and DGAD while Figure 10a shows the false positive window rate produced by each system. FoG-Finder provides a performance increase of 13.4%, 27.0%, 15.4% higher F1 score and 10.7%, 17.4%, 22.6% higher overall accuracy than Bachlin, Mazilu, and DGAD, respectively. FoG-Finder achieves this performance with a significantly lower false positive rate of −96.9%, −120.0%, and −370.8% against these works, respectively. All works achieved a lower overall performance with LOSO analysis when compared with subject-dependent analysis which was expected.

The variability in performance between the patients can be possibly attributed to whether or not the test patient's FoG events and normal gait share part of the feature space of the FoG events and normal gait of the training patients. Since the majority of PD patients will have normal gait present in the 0.5–3Hz band and FoG present in the 3–8Hz band, separating these frequency bands in our FoG-Finder model allowed our model to generalize better than the other works.

6.3.2 FoG Event Level Accuracy—Figure 10b shows the number of correctly identified FoG events for each real-time FoG detection system. Figure 10c shows the false positive treatment rate for Bachlin, Mazilu, DGAD, and FoG-Finder. FoG-Finder achieves similar FoG event detection as the other FoG detection systems while achieving an average LOSO false positive treatment rate reduction of 123.1%, 85.8%, 178.8% when compared with Bachlin, Mazilu, and DGAD, respectively. Given that it is imperative that a real-time FoG detection and treatment system treats every FoG event, we find these results satisfactory that our system could be deployed with unseen patients and still provide treatment for each FoG event.

6.3.3 Treatment Latency—Figure 10d compares the treatment latency of FoG-Finder against the comparison works. FoG-Finder achieves an average treatment latency of 615ms across 10 patients which affirms that FoG-Finder is both a fast and real-time FoG detection and treatment system. Bachlin and DGAD achieve lower latency than FoG-Finder at the expense of much higher false positive treatment rates.

6.4 User Feedback

User feedback concerning the comfort of our FoG-Finder system is important because even if a FoG detection and treatment system is effective at preventing or reducing FoG symptoms, patients may be reluctant to use it if the system is uncomfortable or intrusive. Our study does not have patients answer questions about system comfort since our PD clinicians are conducting a parallel study with the PDVibe3s with a large group of patients (n = 39); this study does receive feedback about device comfort. In this study, patients wear the PDVibe3 devices but not the UG devices. We believe that the user feedback about the comfort of the PDVibe3 devices covers the comfort of our system for the following reasons. First, the PDVibe3 devices are much larger than the UG devices and more likely to be the source of discomfort. Second, the UG devices are placed above the PDVibe3s on the leg where more tissue is present and thus less likely to cause discomfort than the PDVibe3s. Finally, future generations of the FoG-Finder system will see the UG device and PDVibe3 integrated into one device to be worn on the ankle.

A total of 39 patients completed between 1–9 visits where they wore the PDVibe3s on each ankle and received vibration. After each visit, patients were provided with a questionnaire which included questions about PDVibe3 device comfort. Figure 11 shows a breakdown of the positive, neutral, and negative responses to whether or not the PDVibe3 devices were comfortable.

Of the 305 device comfort responses from 39 patients, 93.1% were positive, 4.9% were neutral, and 1.9% were negative. Given these responses, we assert that our FoG-Finder

system does not cause discomfort for the majority of patients and therefore achieves our system requirement of non-intrusiveness.

7 Related Work

7.1 IMU-based Real-time FoG Detection

A viable FoG detection and treatment system can only be said to be real-time if it is validated on portable hardware suitable for use in the real-world. Bachlin et al. [4, 5] proposed a real-time FoG detection and treatment system based on previous threshold-based methods [16, 28] wherein FFT was used to extract the dominant frequencies in the gait frequency and FoG frequency bands for the Y-axis acceleration. The ratio of these frequency bands and the sum of these bands, called the Freezing Index and Power Index, were used to distinguish FoG from normal gait. They used IMUs placed on the left shank, left thigh, and lower trunk. They achieved 73.1% sensitivity and 81.6% specificity under LOSO conditions using 4s windows, and obtained a treatment latency of under 2s. Their system was deployed using auditory cuing as the treatment method of choice. FoG-Finder uses these same frequency bands, but instead of using FFT we use BW filters to maintain the temporal nature of the data. FFT is a powerful tool, but it removes the temporal nature of the data which holds valuable information. Bachlin's method has difficulty distinguishing normal pivot turns from FoG because there is minimal vertical ankle lift with these types of turns.

Mazilu et al. [26] developed a portable FoG detection and treatment system using a smartphone and headphones for auditory cuing. Their features for FoG detection were 7 features (mean, STD, variance, entropy, energy, freezing index, and power index) per IMU axis before feature selection, and they used adaboosted C4.5 trees for FoG detection. Their evaluation was done in both a subject-dependent and LOSO setting using the DAPHNET dataset. For subject-dependent, they reported 98.3% F1 score and 99.8% AUC. However, these results are artificially boosted because they performed random selection of windows when building their training and testing sets meaning significant data leakage was present. The same FoG event could be present in both the training and testing sets, so the their models were not tested with unseen data. Under LOSO conditions, their system achieved 66.2% and 95.3% sensitivity and specificity, respectively. To recap, their system uses 7 time domain and frequency domain features which do not maintain the temporal nature of the data and instead compress each window down to singular values. Such extreme compression must result in the loss of information which is why FoG-Finder uses BW filters to extract frequency domain information whilst still maintaining the temporal nature of the data. The frequency of gait varies overtime so it is important to capture this fact. The performance of Mazilu's system may improve with the addition of thigh and lower back sensors, but this increases the intrusiveness over just two ankle IMUs.

The FoG detection and treatment system by Naghavi et al. [30], DGAD, utilizes two ankle mounted IMUs and they validated that their system is real-time using an Android smartphone. For treatment, the user has the option of auditory cuing using headphones or vibrotactile treatment applied to the wrist using a smart watch. The features they used were filtered sensor readings from each IMU with a single 0.5–8Hz BW filter, and utilized a 5 convolutional layer neural network for FoG detection. They achieved 63.0% and 98.6%

sensitivity and specificity, respectively, in a subject-dependent setting using a dataset of 7 patients. Instead of having a single section containing convolutional layers, FoG-Finder uses two separate groups of convolutional layers running in parallel wherein the sections are provided with either the normal gait band frequency data or the FoG bad frequency data. This separation, along with our additional features to help distinguish pivot turns and straight path FoG events, allowed FoG-Finder to better correctly classify normal gait and FoG events than DGAD.

7.2 IMU-based Offline FoG Detection

There are many IMU-based offline FoG detection works that are not validated on mobile hardware and thus cannot be considered viable at present for real-time, portable FoG detection. The majority of these works can be distinguished by the placement of the IMU(s) for FoG detection. Ankle worn IMUs [3, 7, 10, 27, 39, 42, 49, 53] can be used for FoG detection either alone or with other IMUs placed around the body such as the thigh, waist, or arms. Ankle IMUs can be hidden under pants or socks and have the benefit of being close to the feet where FoG symptoms appear. The addition of other IMUs may be beneficial, but also increases the intrusiveness of the system. Given the effectiveness of FoG-Finder, we believe that ankle IMUs are sufficient for FoG detection. Use of deep CNN-LSTM models or advanced frequency feature extraction methods such as CWT can be used for FoG detection, but our initial exploration of features and models for FoG-Finder found the latency incurred by such methods on mobile hardware to be unacceptable. Our FoG-Finder system is validated on mobile hardware and shown to be practical for real-world deployment.

Waist-worn IMUs [2, 37, 40, 43] can be used for FoG detection, but may be intrusive based on placement. IMUs placed on the back of the waist may be uncomfortable when sitting. Additionally, since the IMU is placed away from the feet where FoG symptoms are the strongest, FoG detection may be less accurate for patients with weak FoG symptoms or patients with full body dyskinesia. Wrist [6] and ear-worn IMUs [34] can also be used to detect FoG. Wrist IMUs can be combined with vibration therapy to the wrist using smart watches and ear IMUs have the benefit of being able to be combined with auditory cuing. However, these systems will be more susceptible to other PD symptoms such as tremor or dyskinesia. As such, we find the use of ankle IMUs more suitable for our system.

7.3 Non-IMU-based FoG Detection

Motion capture systems [9, 13, 35] have been used for FoG classification, but are not practical for real-world deployment since the patient is constrained to a fixed location. These systems are better suited for automating the task of labeling clinical FoG data. Computer vision [19, 21, 31] based approaches using cameras are also suitable methods for automating the FoG labeling process because they lack portability. FoG-Finder is fully portable and therefore more suited for real-world application than these methods.

WiFi-based [47] FoG detection has also been proposed, but is not suitable for uncontrolled environments due to a lack of portability. However, WiFi does not require line-of-sight to the patient and may find practical use in controlled environments such as the patient’s home.

Pressure sensors inside the shoe [24, 36, 46] and pressure mats [45] have been shown to be suitable methods for FoG detection. The three plantar pressure sensor systems, Pardoel et al. [36], Marcante et al. [24], and Shalin [46] are suitable for real-world environments but were not evaluated under real-time constraints on portable hardware. Additionally, Pardoel et al. and Marcante et al. only had 94.5% and 90% FoG event level accuracy which means their systems are not in-situ. Shalin et al. only achieved an F1 score of 31% and does not yet have the performance needed to reliably detect FoG. These systems also require the patient to either wear specialized shoes or shoe inserts. IMU-based FoG detection allows patients to wear their preferred choice of footwear. Pressure mats are not portable, but may serve for automatic labeling in clinical environments.

EEG [17, 18], EMG [8], and skin conductance [25] can be used for FoG Detection. These systems require skin contact and are more intrusive than IMUs. Also, EEG systems are more difficult to disguise making them less practical for real-world applications. However, these systems have an advantage over IMU-based FoG detection systems since pure akinesia FoG events, FoG events where the patient has no movement, are identical to intentionally standing still in the time domain and frequency domain. Patients that only experience akinesia FoG may need more intrusive sensor platforms for FoG detection.

8 Conclusion

FoG is a common and dangerous symptom of PD that increases the risk individuals will fall and sustain injury. To address this problem, we presented FoG-Finder, a closed-loop, portable, and real-time FoG detection and treatment system. To accurately detect FoG, we transformed IMU data into the known frequency ranges that dominate healthy gait (0.5–3Hz) and FoG (3–8Hz) using BW filters. Our FoG-Finder CNN model extracts feature representations for these frequency bands separately which provides superior performance to past works that combine these frequency bands. Our system was able to achieve 13.4% higher F1 score and 10.7% higher overall accuracy compared with other validated real-time FoG detection and treatment systems in a LOSO setting. Additionally, FoG-Finder achieved an average treatment latency of 427ms and 615ms for subject-dependent and LOSO settings, respectively, making it a viable system to treat FoG in the real-world. FoG-Finder was validated on our FoG dataset containing 716 freezes from 11 patients. Our dataset will be made publicly available at the conclusion of our study.

Acknowledgments

This work was funded through the National Institute of Health, grant NIH NINDS (R01NS120560). User responses shown in Section 6.4 were collected in a study funded by the Michael J. Fox Foundation (MJFF 16496).

References

[1]. Aggarwal Rajeev, Pretzer Ingrid, Winfree KyleN, Agrawal SunilK, and Behari Madhuri. 2019. Clinical outcomes of step-synchronized vibration training in patients of Parkinson’s disease with freezing of gait. Annals of Movement Disorders 2 (01 2019), 15.

[2]. Ahlrichs Claas, Monsonís Albert Samà, Lawo Michael, Cabestany Joan, Rodríguez-Martín Daniel, Pérez Carlos, Sweeney Dean, Quinlan Leo, ÓLaighin Gearóid, Counihan Timothy, Browne Patrick, Lewy Hadas, Vainstein Gabriel, Costa Alberto, Annicchiarico Roberta, Alcaine Sheila,

Mestre Berta, Quispe Paola, Bayés Angels, and Rodríguez-Molinero Alejandro. 2015. Detecting freezing of gait with a tri-axial accelerometer in Parkinson's disease patients. Medical & Biological Engineering & Computing 54 (10 2015).

[3]. Assam Roland and Seidl T. 2014. Prediction of freezing of gait from Parkinson's Disease movement time series using conditional random fields. In HealthGIS '14.

[4]. Bächlin Marc,Hausdorff Jeffrey M., Roggen Daniel, Giladi Nir, Plotnik Meir, and Tröster Gerhard. 2009. Online Detection of Freezing of Gait in Parkinson's Disease Patients: A Performance Characterization. In Proceedings of the Fourth International Conference on Body Area Networks (Los Angeles, California) (BodyNets '09). ICST (Institute for Computer Sciences, Social-Informatics and Telecommunications Engineering), Brussels, BEL, Article 11, 8 pages.

[5]. Bachlin Marc, Plotnik Meir, Roggen Daniel, Maidan Inbal, Hausdorff Jeffrey M., Giladi Nir, and Troster Gerhard. 2010. Wearable Assistant for Parkinson's Disease Patients With the Freezing of Gait Symptom. IEEE Transactions on Information Technology in Biomedicine 14, 2 (2010), 436–446. [PubMed: 19906597]

[6]. Camps Julià, Samà Albert, Martín Mario, Martín Daniel Rodríguez, Pérez-López Carlos, Aróstegui Juan-Manuel Moreno, Cabestany Joan, Català Andreu, Alcaine Sheila, Mestre Berta, Prats Anna, Crespo-Maraver Maria C., Counihan Timothy J., Browne Patrick, Quinlan Leo R., Laighin Gearóid Ó, Sweeney Dean, Lewy Hadas, Vainstein Gabriel, Costa Alberto, and Annicchiarico Roberta. 2018. Deep learning for freezing of gait detection in Parkinson's disease patients in their homes using a waist-worn inertial measurement unit. Knowl. Based Syst 139 (2018), 119–131.

[7]. Cole Bryan T., Roy Serge H., and Nawab S. Hamid. 2011. Detecting freezing-of-gait during unscripted and unconstrained activity. In 2011 Annual International Conference of the IEEE Engineering in Medicine and Biology Society. 5649–5652.

[8]. Cole Bryan T., Roy Serge H., and Nawab S. Hamid. 2011. Detecting freezing-of-gait during unscripted and unconstrained activity. In 2011 Annual International Conference of the IEEE Engineering in Medicine and Biology Society. 5649–5652.

[9]. Delval Arnaud, Snijders Anke, Weerdesteyn Vivian, Duysens Jacques, Defebvre Luc, Giladi Nir, and Bloem Bas. 2010. Objective Detection of Subtle Freezing of Gait Episodes in Parkinson's Disease. Movement disorders : official journal of the Movement Disorder Society 25 (08 2010), 1684–93. [PubMed: 20544715]

[10]. Djurić-Jovičić Milica D., Jovičić Nenad S., Radovanović Saša M., Stanković Iva D., Popović Mirjana B., and Kostić Vladimir S.. 2014. Automatic Identification and Classification of Freezing of Gait Episodes in Parkinson's Disease Patients. IEEE Transactions on Neural Systems and Rehabilitation Engineering 22, 3 (2014), 685–694. [PubMed: 24235277]

[11]. Donovan S, Lim C, Diaz N, Browner N, Rose P, Sudarsky LR, Tarsy D, Fahn S, and Simon DK. 2011. Laserlight cues for gait freezing in Parkinson's disease: An open-label study. Parkinsonism & Related Disorders 17, 4 (2011), 240–245. [PubMed: 20817535]

[12]. Fasano Alfonso, Laganiere Simon, Lam Susy, and Fox Michael. 2016. Lesions causing freezing of gait localize to a cerebellar functional network. Annals of neurology 81 (12 2016).

[13]. Filtjens Benjamin, Ginis Pieter, Nieuwboer Alice, Slaets Peter, and Vanrumste Bart. 2021. Automated freezing of gait assessment with marker-based motion capture and deep learning approaches expert-level detection.

[14]. Giladi N, Treves TA, Simon ES, Shabtai H, Orlov Y, Kandinov B, Paleacu D, and Korczyn AD. 2001. Freezing of gait in patients with advanced Parkinson's disease. Journal of Neural Transmission 108, 1 (01 Jan 2001), 53–61. [PubMed: 11261746]

[15]. Gilat Moran. 2019. How to Annotate Freezing of Gait from Video: A Standardized Method Using Open-Source Software. Journal of Parkinson's Disease 9 (09 2019), 1–4.

[16]. Han Jong Hee, Lee Won Jin, Ahn Tae Beom, Jeon Beom Suk, and Park Kwang Suk. 2003. Gait analysis for freezing detection in patients with movement disorder using three dimensional acceleration system. In Proceedings of the 25th Annual International Conference of the IEEE Engineering in Medicine and Biology Society (IEEE Cat. No.03CH37439), Vol. 2. 1863–1865 Vol.2.

[17]. Handojoseno Ardi, Shine James, Nguyen Tuan, Tran Yvonne, Lewis Simon, and Nguyen Hung. 2014. Analysis and Prediction of the Freezing of Gait Using EEG Brain Dynamics. IEEE Transactions on Neural Systems and Rehabilitation Engineering (12 2014).

[18]. Handojoseno Aluysius Maria Ardi, Naik Ganesh R., Gilat Moran, Shine James M., Nguyen Tuan Nghia, Ly Quynh Tran, Lewis Simon J. G., and Nguyen Hung Tan. 2018. Prediction of Freezing of Gait in Patients with Parkinson's Disease Using EEG Signals. Studies in health technology and informatics 246 (2018), 124–131. [PubMed: 29507265]

[19]. Hu Kun, Wang Zhiyong, Mei Shaohui, Ehgoetz Martens Kaylena A., Yao Tingting, Lewis Simon J. G., and Feng David Dagan. 2020. Vision-Based Freezing of Gait Detection With Anatomic Directed Graph Representation. IEEE Journal of Biomedical and Health Informatics 24, 4 (2020), 1215–1225. [PubMed: 31217134]

[20]. Ishii Mitsuaki and Okuyama Kohei. 2017. Characteristics associated with freezing of gait in actual daily living in Parkinson's disease. Journal of physical therapy science 29, 12 (Dec 2017), 2151–2156. [PubMed: 29643593]

[21]. Khan Taha, Westin Jerker, and Dougherty Mark. 2013. Motion Cue Analysis for Parkinsonian Gait Recognition. The open biomedical engineering journal 7 (01 2013), 1–8. [PubMed: 23407764]

[22]. King Lauren, Almeida Quincy J., and Ahonen Heidi. 2009. Short-term effects of vibration therapy on motor impairments in Parkinson's disease. NeuroRehabilitation 25 4 (2009), 297–306. [PubMed: 20037223]

[23]. Lynall Robert, Zukowski Lisa, Plummer Prudence, and Mihalik Jason. 2016. Reliability and Validity of the Protokinetics Movement Analysis Software in Measuring Center of Pressure during Walking. Gait & Posture 52 (12 2016).

[24]. Marcante Andrea, Di Marco Roberto, Gentile Giovanni, Pellicano Clelia, Assogna Francesca, Pontieri Francesco Ernesto, Spalletta Gianfranco, Macchiusi Lucia, Gatsios Dimitris, Giannakis Alexandros, Chondrogiorgi Maria, Konitsiotis Spyridon, Fotiadis Dimitrios I., and Antonini Angelo. 2021. Foot Pressure Wearable Sensors for Freezing of Gait Detection in Parkinson's Disease. Sensors 21, 1 (2021).

[25]. Mazilu Sinziana, Calatroni Alberto, Gazit Eran, Mirelman Anat, Hausdorff Jeffrey M., and Tröster Gerhard. 2015. Prediction of Freezing of Gait in Parkinson's From Physiological Wearables: An Exploratory Study. IEEE Journal of Biomedical and Health Informatics 19, 6 (2015), 1843–1854. 10.1109/JBHI.2015.2465134 [PubMed: 26259206]

[26]. Mazilu Sinziana, Hardegger Michael, Zhu Zack, Roggen Daniel, Tröster Gerhard, Plotnik Meir, and Hausdorff Jeffrey M.. 2012. Online detection of freezing of gait with smartphones and machine learning techniques. In 2012 6th International Conference on Pervasive Computing Technologies for Healthcare (PervasiveHealth) and Workshops. 123–130.

[27]. Mekruksavanich Sakorn and Jitpattanakul Anuchit. 2021. Detection of Freezing of Gait in Parkinson's Disease by Squeeze-and-Excitation Convolutional Neural Network with Wearable Sensors. In 2021 15th International Conference on Open Source Systems and Technologies (ICOSST). 1–5.

[28]. Moore Steven T., MacDougall Hamish G., and Ondo William G.. 2008. Ambulatory monitoring of freezing of gait in Parkinson's disease. Journal of Neuroscience Methods 167, 2 (2008), 340–348. [PubMed: 17928063]

[29]. Catherine MPH, Erickson-Davis Cordelia, Rose PT, Walde-Douglas Maria, PhD MD, Wielinski Catherine, Wichmann Rose, Walde-Douglas Maria, and Parashos Sotirios. 2005. Falls and injuries resulting from falls among patients with Parkinson's disease and other Parkinsonian syndromes. Movement Disorders 20 (04 2005), 410–415. [PubMed: 15580552]

[30]. Naghavi Nader and Wade Eric. 2022. Towards Real-Time Prediction of Freezing of Gait in Patients With Parkinson's Disease: A Novel Deep One-Class Classifier. IEEE Journal of Biomedical and Health Informatics 26, 4 (2022), 1726–1736. [PubMed: 34375292]

[31]. Nieto-Hidalgo Mario, Ferrndez-Pastor Francisco Javier, Valdivieso-Sarabia Rafael J., Mora-Pascual Jernimo, and Garca-Chamizo Juan Manuel. 2016. A Vision Based Proposal for Classification of Normal and Abnormal Gait Using RGB Camera. J. of Biomedical Informatics 63, C (oct 2016), 82–89. [PubMed: 27498069]

[32]. Nombela Cristina, Hughes Laura E., Owen Adrian M., and Grahn Jessica A.. 2013. Into the groove: Can rhythm influence Parkinson's disease? Neuroscience & Biobehavioral Reviews 37, 10, Part 2 (2013), 2564–2570. [PubMed: 24012774]

[33]. Nutt John, Bloem Bas, Giladi Nir, Hallett Mark, Horak Fay, and Nieuwboer Alice. 2011. Freezing of gait: Moving forward on a mysterious clinical phenomenon. Lancet neurology 10 (08 2011), 734–44. [PubMed: 21777828]

[34]. Oishi Nobuyuki, Heimler Benedetta, Pellatt Lloyd, Plotnik Meir, and Roggen Daniel. 2021. Detecting Freezing of Gait with Earables Trained from VR Motion Capture Data. In 2021 International Symposium on Wearable Computers (Virtual, USA) (ISWC '21). Association for Computing Machinery, New York, NY, USA, 33–37.

[35]. Oishi Nobuyuki, Heimler Benedetta, Pellatt Lloyd, Plotnik Meir, and Roggen Daniel. 2021. Detecting Freezing of Gait with Earables Trained from VR Motion Capture Data. In 2021 International Symposium on Wearable Computers (Virtual, USA) (ISWC '21). Association for Computing Machinery, New York, NY, USA, 33–37.

[36]. Pardoel Scott, Nantel Julie, Kofman Jonathan, and Lemaire Edward D.. 2022. Prediction of Freezing of Gait in Parkinson's Disease Using Unilateral and Bilateral Plantar-Pressure Data. Frontiers in Neurology 13 (2022).

[37]. Pepa L, Ciabattoni L, Verdini F, Capecci M, and Ceravolo MG. 2014. Smartphone based Fuzzy Logic freezing of gait detection in Parkinson's Disease. In 2014 IEEE/ASME 10th International Conference on Mechatronic and Embedded Systems and Applications (MESA). 1–6.

[38]. Pereira Marcelo P., Gobbi Lilian T.B., and Almeida Quincy J.. 2016. Freezing of gait in Parkinson's disease: Evidence of sensory rather than attentional mechanisms through muscle vibration. Parkinsonism & Related Disorders 29 (2016), 78–82. [PubMed: 27245918]

[39]. Pham Thuy T., Moore Steven T., Lewis Simon John Geoffrey, Nguyen Diep N., Dutkiewicz Eryk, Fuglevand Andrew J., McEwan Alistair L., and Leong Philip H.W.. 2017. Freezing of Gait Detection in Parkinson's Disease: A Subject-Independent Detector Using Anomaly Scores. IEEE Transactions on Biomedical Engineering 64, 11 (2017), 2719–2728. [PubMed: 28186875]

[40]. Pham Thuy T., Moore Steven T., Lewis Simon John Geoffrey, Nguyen Diep N., Dutkiewicz Eryk, Fuglevand Andrew J., McEwan Alistair L., and Leong Philip H.W.. 2017. Freezing of Gait Detection in Parkinson's Disease: A Subject-Independent Detector Using Anomaly Scores. IEEE Transactions on Biomedical Engineering 64, 11 (2017), 2719–2728. [PubMed: 28186875]

[41]. Pycroft Laurie, Stein John, and Aziz Tipu. 2018. Deep brain stimulation: An overview of history, methods, and future developments. Brain and neuroscience advances 2 (12 Dec 2018), 2398212818816017–2398212818816017.

[42]. Rezvanian Saba and Lockhart Thurmon E.. 2016. Towards Real-Time Detection of Freezing of Gait Using Wavelet Transform on Wireless Accelerometer Data. Sensors 16, 4 (2016).

[43]. Rodríguez-Martín Daniel, Monsonís Albert Samà, Pérez Carlos, Català Andreu, Arostegui Joan, Cabestany Joan, Angels Bayés, Alcaine Sheila, Mestre Berta, Prats Anna, Maraver Maria Cruz Crespo, Counihan Timothy, Browne Patrick, Quinlan Leo, ÓLaighin Gearóid, Sweeney Dean, Lewy Hadas, Azuri Joseph, Vainstein Gabriel, and Rodríguez-Molinero Alejandro. 2017. Home detection of freezing of gait using Support Vector Machines through a single waist-worn triaxial accelerometer. PLOS ONE 12 (02 2017), e0171764. [PubMed: 28199357]

[44]. Schrader C, Capelle H-H, Kinfe TM, Blahak C, Bäzner H, Lütjens G, Dressler D, and Krauss JK. 2011. GPi-DBS may induce a hypokinetic gait disorder with freezing of gait in patients with dystonia. Neurology 77, 5 (2011), 483–488. [PubMed: 21775741]

[45]. Shah Jesal, Pillai Lakshmi, Williams David K., Doerhoff Shannon M., Larson-Prior Linda, Garcia-Rill Edgar, and Virmani Tuhin. 2018. Increased foot strike variability in Parkinson's disease patients with freezing of gait. Parkinsonism & Related Disorders 53 (2018), 58–63. [PubMed: 29773512]

[46]. Shalin Gaurav, Pardoel Scott, Lemaire Edward, Nantel Julie, and Kofman Jonathan. 2021. Prediction and detection of freezing of gait in Parkinson's disease from plantar pressure data using long short-term memory neural-networks. Journal of NeuroEngineering and Rehabilitation 18 (11 2021).

[47]. Tahir Ahsen, Ahmad Jawad, Shah Syed Aziz, Morison Gordon, Skelton Dawn A., Larijani Hadi, Abbasi Qammer H., Imran Muhammad Ali, and Gibson Ryan M.. 2019. WiFreeze:

Multiresolution Scalograms for Freezing of Gait Detection in Parkinson's Leveraging 5G Spectrum with Deep Learning. Electronics 8, 12 (2019).

[48]. Trenkwalder Claudia, Kuoppamäki Mikko, Vahteristo Mikko, Müller Thomas, and Ellmén Juha. 2019. Increased dose of carbidopa with levodopa and entacapone improves "off" time in a randomized trial. Neurology 92, 13 (2019), e1487–e1496. [PubMed: 30824559]

[49]. Wang Fu-Cheng, Li You-Chi, Kuo Tien-Yun, Chen Szu-Fu, and Lin Chin-Hsien. 2021. Real-Time Detection of Gait Events by Recurrent Neural Networks. IEEE Access 9 (2021), 134849–134857.

[50]. Weytjens Hans and Weerdt Jochen. 2020. Process Outcome Prediction: CNN vs. LSTM (with Attention). 321–333.

[51]. Willis AW, Roberts E, Beck JC, Fiske B, Ross W, Savica R, Van Den Eeden SK, Tanner CM, Marras C, Alcalay Roy, Schwarzschild Michael, Racette Brad, Chen Honglei, Church Tim, Wilson Bill, Doria James M., and on behalf of the Parkinson's Foundation P4 Group. 2022. Incidence of Parkinson disease in North America. npj Parkinson's Disease 8, 1 (15 Dec 2022), 170.

[52]. Winfree Kyle N., Pretzer-Aboff Ingrid, Hilgart David, Aggarwal Rajeev, Behari Madhuri, and Agrawal Sunil K.. 2013. The Effect of Step-Synchronized Vibration on Patients With Parkinson's Disease: Case Studies on Subjects With Freezing of Gait or an Implanted Deep Brain Stimulator. IEEE Transactions on Neural Systems and Rehabilitation Engineering 21, 5 (2013), 806–811. 10.1109/TNSRE.2013.2250308 [PubMed: 23508270]

[53]. Xia Yi, Zhang Jun, Ye Qiang, Cheng Nan, Lu Yixiang, and Zhang Dexiang. 2018. Evaluation of deep convolutional neural networks for detection of freezing of gait in Parkinson's disease patients. Biomedical Signal Processing and Control 46 (2018), 221–230.

[54]. Zhao Hongyang, Wang Shuangquan, Zhou Gang, and Zhang Daqing. 2019. Ultigesture: A wristband-based platform for continuous gesture control in health-care. Smart Health 11 (2019), 45–65. Emerging Healthcare Technologies.

CCS Concepts

• **Human-centered computing** → *Ubiquitous and mobile computing systems and tools*;
• **Applied computing** → **Consumer health**.

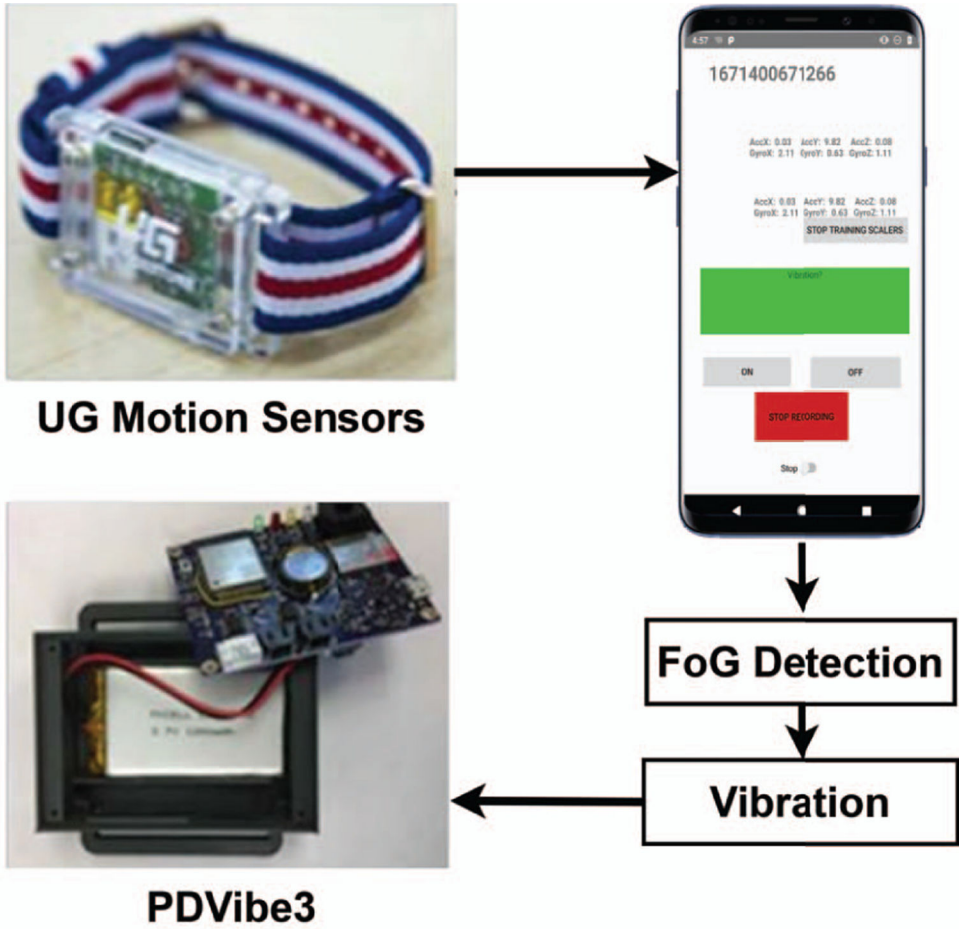

Figure 1:
Closed-loop FoG-Finder System

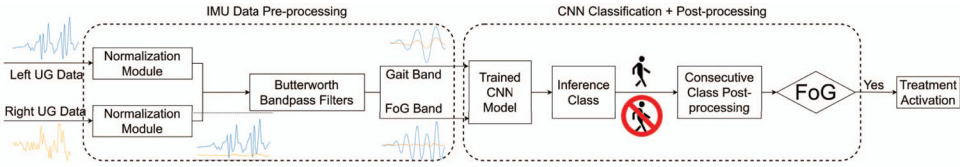

Figure 2:
FoG-Finder Data Flow

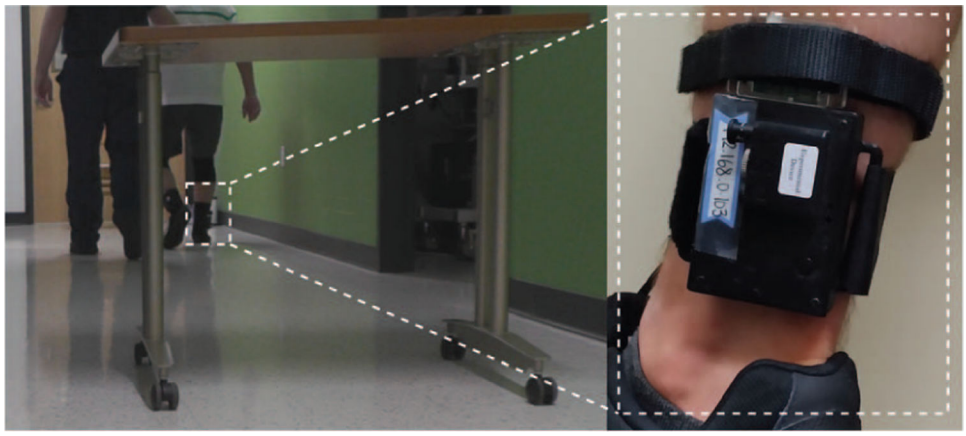

Figure 3:
UG and PDVibe3 Placement on Ankle

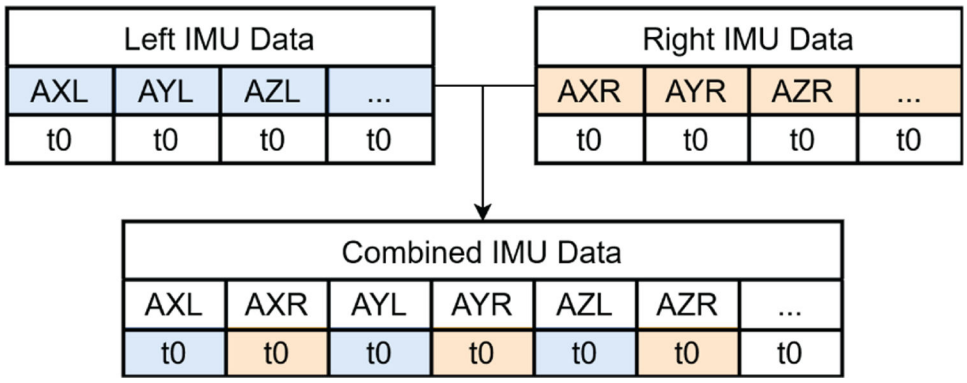

Figure 4:
Time Domain Feature Combination

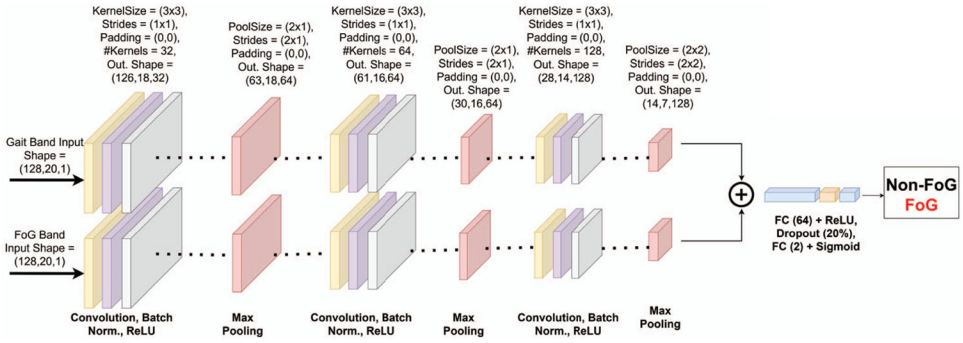

Figure 5:
FoG-Finder Multi-input CNN Design

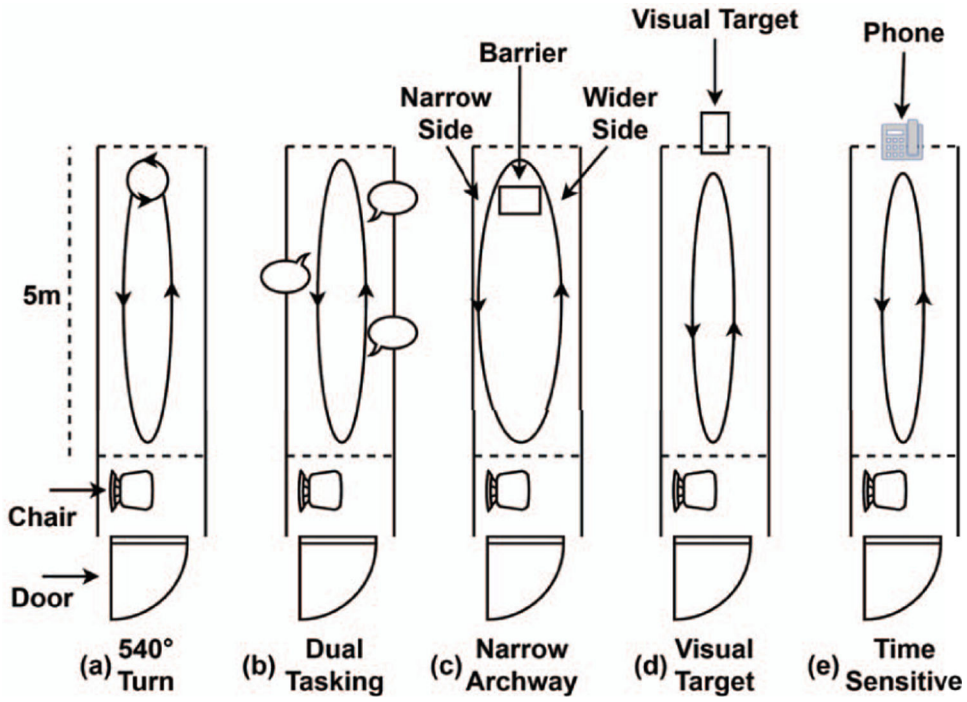

Figure 6:
Environmental Setup for the Top 5 FoG Triggering Scenarios

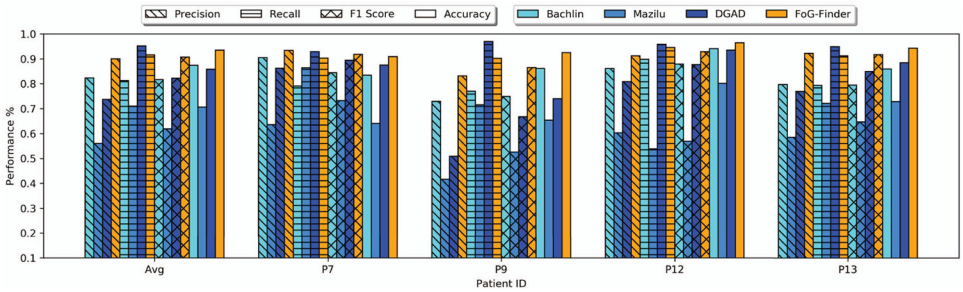

Figure 7:
Subject-Dependent Window Level Performance

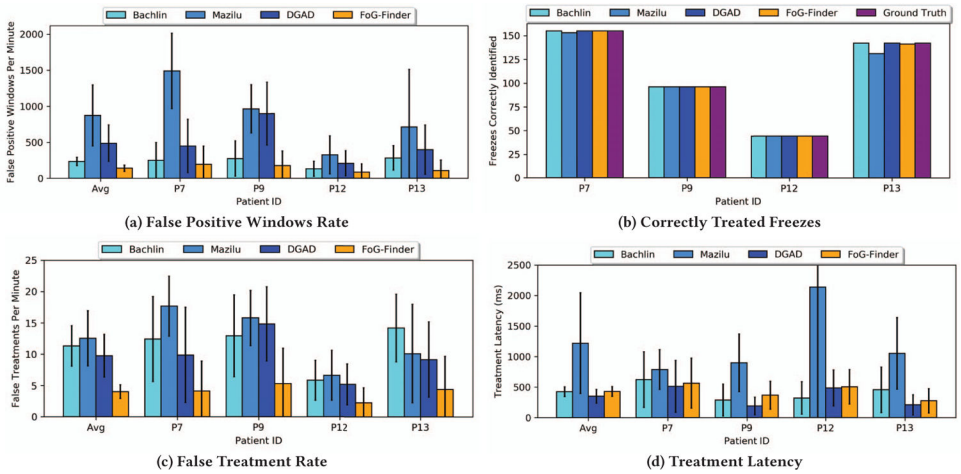

Figure 8:
Subject-Dependent Performance Evaluation

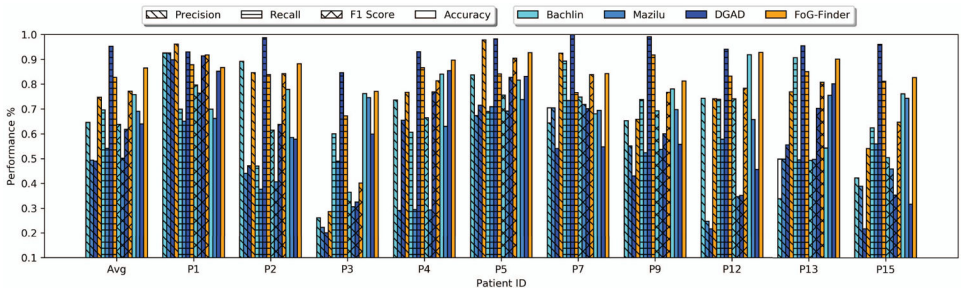

Figure 9:
Leave-One-Subject-Out Window Level Performance

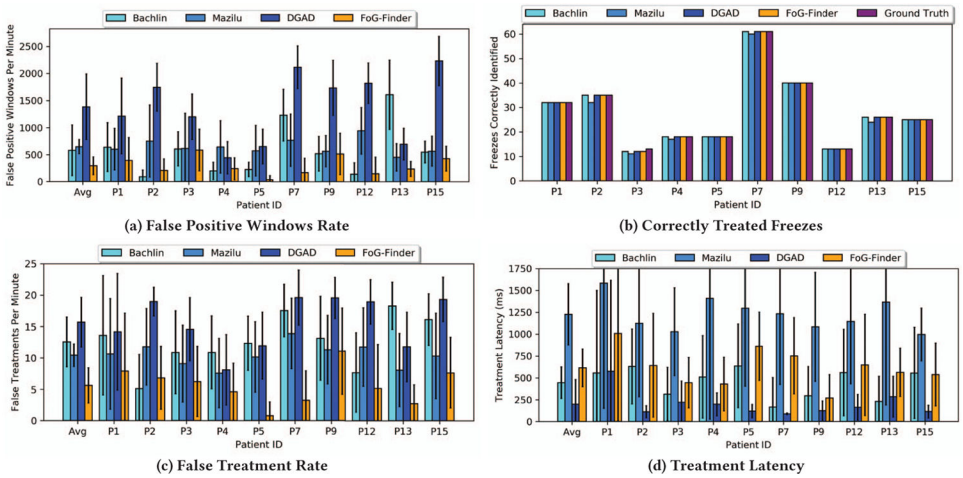

Figure 10:
Leave-One-Subject-Out Performance Comparison

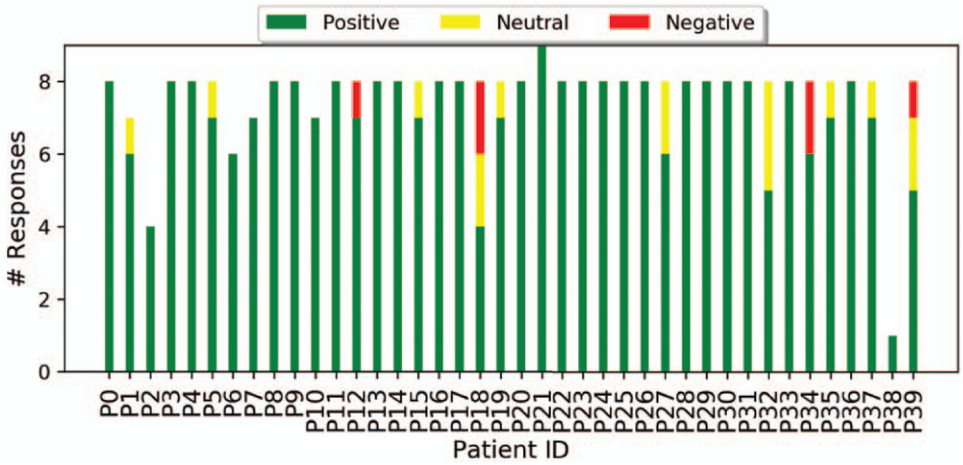

Figure 11:
Patient Responses Concerning Device Comfort

Table 1:

Overview of Patient Data

Patient ID	Test Month	Phase #	Visit #	Medication	Gait Time (s)	FoG Time (s)	Total Time (s)	FoG %	# FoG Events	Avg. FoG Length (s)
P1	May 2021	1	1	OFF	227.767	749.034	941.901	79.52	33	22.698 ± 28.331
P2	June 2021	1	1	OFF	477.693	201.070	667.130	30.14	38	5.291 ± 7.369
P3	June 2021	1	1	OFF	451.665	39.166	490.831	7.98	21	1.865 ± 0.714
P4	July 2021	1	1	OFF	387.561	90.501	459.496	19.7	20	4.525 ± 4.756
P5	September 2021	1	1	OFF	292.063	169.100	435.263	38.85	19	8.900 ± 9.344
P6	November 2021	1	1	OFF	427.396	0.000	427.396	0.00	0	0.000 ± 0.000
P7	June 2022	2	1	ON	430.290	262.694	646.438	40.64	62	5.386 ± 4.566
P7	June 2022	2	2	ON	1047.812	817.099	1823.870	44.80	156	5.23 ± 5.208
P9	June 2022	2	1	ON	453.969	145.280	591.891	24.55	40	3.632 ± 2.371
P9	June 2022	2	2	ON	1559.330	343.895	1816.203	18.93	100	3.439 ± 2.724
P12	July 2022	2	1	ON	485.952	70.021	555.973	12.59	13	5.386 ± 4.566
P12	July 2022	2	2	ON	1590.863	469.805	2059.351	22.81	43	10.926 ± 20.825
P13	July 2022	2	1	ON	539.886	130.267	670.153	19.44	27	4.825 ± 4.677
P13	July 2022	2	2	ON	1615.901	553.971	2056.643	26.94	119	4.655 ± 5.181
P15	August 2022	2	1	ON	495.526	72.825	547.647	13.30	25	2.913 ± 1.423
Stats	2021 - Present	1 & 2	1 & 2	OFF & ON	Sum: 10056.278	Sum: 4114.728	Sum: 13762.790	Avg: 40.92	Sum: 716	Avg: 5.747 ± 10.001

IEEE Int Conf Connect Health Appl Syst Eng Technol. Author manuscript; available in PMC 2023 September 21.